

## Second-order Raman scattering by confined optical phonons and interface vibrational modes in GaAs-AlAs superlattices

A. K. Sood,\* J. Menéndez, M. Cardona, and K. Ploog  
 Max-Planck-Institut für Festkörperforschung, Heisenbergstrasse 1,  
 D-7000 Stuttgart 80, Federal Republic of Germany

(Received 15 March 1985)

The second-order Raman spectrum of the confined GaAs-like optical phonons in a GaAs-AlAs superlattice is reported. For laser energies in resonance with the first exciton in the GaAs quantum wells, the experiments show a series of sharp peaks that can be attributed to combinations of confined phonons of  $A_1$  symmetry. An additional broader peak corresponds to the combination of the GaAs-like and AlAs-like interface vibrational modes previously reported in the first-order spectra. The resonance profile of the overtones and combinations of confined phonons is also presented.

Under resonant conditions, Raman scattering by longitudinal optical (LO) phonons in polar semiconductors can be observed in scattering configurations which are forbidden according to the dipole selection rules.<sup>1</sup> This phenomenon is due to the  $\mathbf{q}$ -dependent ( $\mathbf{q}$  is the phonon wave vector) contribution of the Fröhlich electron-phonon interaction to the Raman efficiency. While the phonon wave vector is small in first-order scattering<sup>2</sup> due to conservation of crystal momentum, the pairs of phonons which participate in the corresponding second-order process are only subject to the restriction that the *sum* of their wave vectors must be nearly zero. Thus, phonons with arbitrary wave vectors can participate in second-order Raman scattering. This additional degree of freedom allows for double resonances, which dramatically enhance the Raman efficiency; theory<sup>3</sup> predicts the Fröhlich-interaction-induced scattering by two LO phonons to be stronger than its first-order counterpart. This has actually been observed in GaP,<sup>4</sup> CdTe,<sup>5</sup> and GaAs.<sup>6</sup> Only for the case of impurity-induced intraband Fröhlich Raman scattering by LO phonons<sup>2</sup> (a process which is formally similar to Raman scattering by two LO phonons<sup>5</sup>) first- and second-order intensities become of comparable magnitude.

The results obtained for bulk materials suggest that Raman scattering by two LO phonons is an excellent candidate for the study of second-order Raman scattering in semiconductor superlattices. This paper reports for the first time such measurements for a GaAs-AlAs superlattice.

Raman experiments in the backscattering configuration were performed for (001)-oriented GaAs-AlAs superlattices grown by molecular-beam epitaxy. We present here results for one sample with  $d_1=20$  Å and  $d_2=60$  Å ( $d_1$  and  $d_2$  are the thicknesses of the GaAs and AlAs slabs, respectively). The period  $d=d_1+d_2$  was repeated 400 times. The results for other samples with different  $d_1$  and  $d_2$  are qualitatively similar to the ones given here. The temperature of the sample during the measurements was  $\sim 10$  K. The spectra were excited with a DCM dye laser (supplied by Lamda Physik, Göttingen, FRG) pumped with a cw Ar<sup>+</sup> laser. The scattered light was analyzed with a Jarrell Ash double monochromator and detected by photon counting.

Figure 1 shows the first-order Raman spectrum in the region corresponding to the optical phonons of GaAs. The peaks labeled  $LO_m$  correspond to the confined (sometimes improperly called "folded") optical phonons.<sup>7,8</sup> These are

modes localized in the GaAs slabs, equivalent to those vibrations in the bulk material whose wave vector is given by  $q = m\pi/d_1$ . In the  $D_{2d}$  point group of the superlattice, the odd values of  $m$  correspond to phonons belonging to the  $B_2$  representation, while the even values denote  $A_1$ -type phonons. The peak  $IF_1$  has been attributed to an interface mode.<sup>9</sup> In contrast with the confined phonons, which are localized in either slab, the interface vibrations imply some polarization in both materials. A second interface mode, which we call  $IF_2$ , can be seen with a Raman shift corresponding to the optical phonon frequencies in AlAs. This peak resonates strongly with the excitons localized in the GaAs slabs,<sup>9</sup> thus demonstrating the interface character of the vibration.

The  $A_1$  modes dominate the spectra taken with the laser light in resonance with the first electron-heavy-hole exciton in the GaAs quantum wells (solid line in Fig. 1). The  $B_2$  modes can only be seen far from resonance and in a scatter-

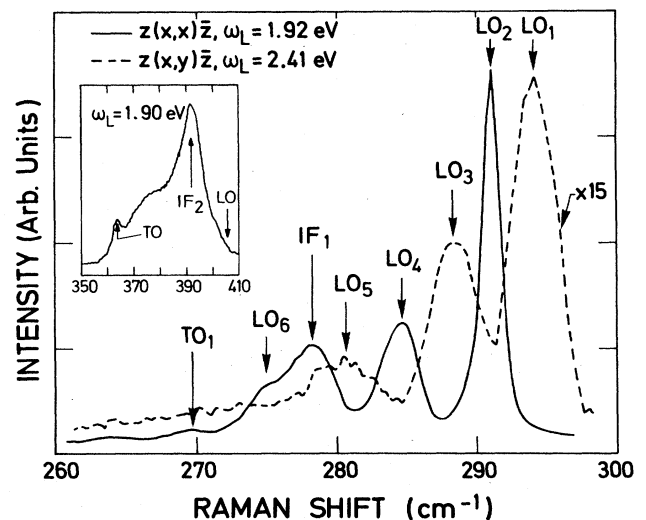


FIG. 1. First-order Raman spectrum of the confined LO phonons in a GaAs-AlAs superlattice with  $d_1=20$  Å,  $d_2=60$  Å. The different peak widths are due to the different spectrometer resolutions in the resonant case (solid line) and the off-resonance case (dashed line). The inset shows the Raman spectrum in the region of the AlAs-like optical phonons (Refs. 8 and 9).

ing configuration which is allowed for Raman scattering induced by the deformation-potential-type electron-phonon interaction.<sup>1</sup> This alternation of the modes is due to their different types of coupling with the electronic system. The most strongly resonant contribution to the Raman efficiency is given by the intraband matrix elements of the Fröhlich electron-phonon interaction.<sup>1,8</sup> These matrix elements are of the form

$$\int_{-d_1/2}^{d_1/2} dz \cos^2 \beta z \times \begin{cases} \sin(m\pi z/d_1) & (m=1,3,5, \dots) \\ \cos(m\pi z/d_1) & (m=2,4,6, \dots) \end{cases} \quad (1)$$

since the electronic wave functions are of the form  $\psi \propto \cos(\beta z)$ , where  $\beta^2 = 2mE/\hbar^2$ ,  $E$  being the electron-level energy. The Fröhlich potential  $V_F$  can be deduced by noting that the relative atomic displacements, given by<sup>10</sup>

$$\begin{aligned} u_{rel} &\propto \cos(m\pi z/d_1) \quad (B_2 \text{ modes, } m \text{ odd}), \\ u_{rel} &\propto \sin(m\pi z/d_1) \quad (A_1 \text{ modes, } m \text{ even}), \end{aligned} \quad (2)$$

are proportional to the gradient of  $V_F$ . Equation (1) means that the matrix element cancels for  $B_2$  modes, thus explaining why only  $A_1$  modes are seen in resonance.

Figure 2 shows Raman spectra in the region corresponding to the second-order spectrum of the GaAs optical branches. The spectrum in the lower part of the figure was taken near resonance. The Raman structure rides on a photoluminescence background. The most interesting feature

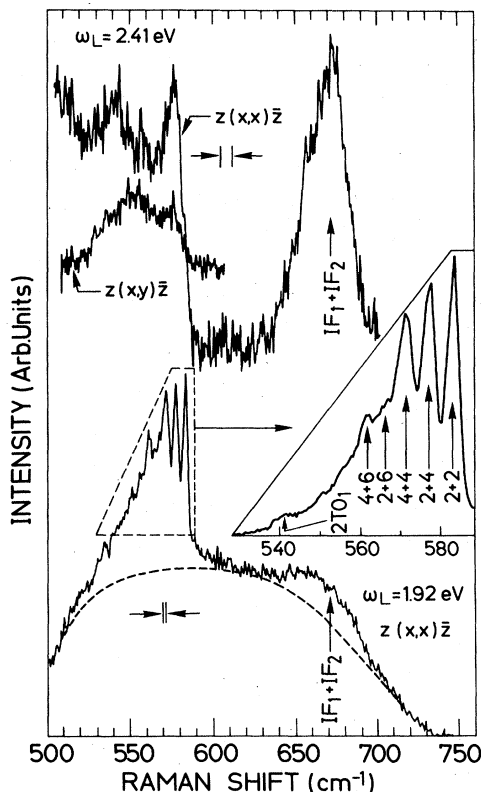


FIG. 2. Second-order Raman spectrum of the same superlattice as in Fig. 1. The numbers assigned to the peaks in the inset correspond to the subindexes in Fig. 1.

(also shown in the triangular inset) is the set of sharp peaks which we attribute to combinations of the peaks seen in Fig. 1. However, as can be observed by comparing the measured frequencies for the first- and second-order spectra, the combinations  $LO_1 + LO_1$  and  $LO_1 + LO_2$  are missing. In fact, all the second-order peaks can be explained as combinations of  $A_1$  modes ( $m$  even). The absence of  $B_2$  modes in the resonance spectrum is due to the same matrix-element cancellation discussed for the first-order spectra. The theoretical expression for the second-order Raman efficiency<sup>3</sup> has an additional intraband matrix element of the Fröhlich interaction, i.e., it is of fourth order in perturbation theory,<sup>3</sup> because two phonons must be created. Thus, the only nonvanishing contributions are those in which neither of the two Fröhlich matrix elements involve  $B_2$  phonons. Figure 3 shows the resonance behavior of the  $A_1$ -phonon combinations. It displays the typical characteristics of the double-resonance effects:<sup>3,5,11</sup> a dominant outgoing resonance and an asymmetric general shape, with stronger scattering efficiencies to higher energies. This is due to the fact that double resonances are only possible when the laser frequency is in the continuum ( $\omega_L > \omega_1 + 2\Omega_{LO}$ , where  $\omega_L$  is the laser frequency,  $\omega_1$  the exciton energy, and  $\Omega_{LO}$  the LO-phonon frequency). All these aspects of the Raman scattering by two confined phonons closely resemble what occurs in bulk material. However, as found in the first-order spectra,<sup>8</sup> the peaks in resonance are seen for all scattering configurations.

An additional interesting feature in the second-order spectra is the broad peak labeled  $IF_1 + IF_2$ . This peak exactly corresponds to the sum of the interface modes  $IF_1$  and  $IF_2$  of Fig. 1.

In the off-resonance spectra (upper part of Fig. 2) we expect to see all possible combinations of confined phonons because now the contribution of the deformation-potential interaction cannot be neglected. However, the combinations  $LO_1 + LO_1$  and  $LO_2 + LO_2$  also seem to be missing in the off-resonance case. We believe that this is an apparent effect due to the shift of the second-order Raman peak as a function of the laser energy. This phenomenon has also

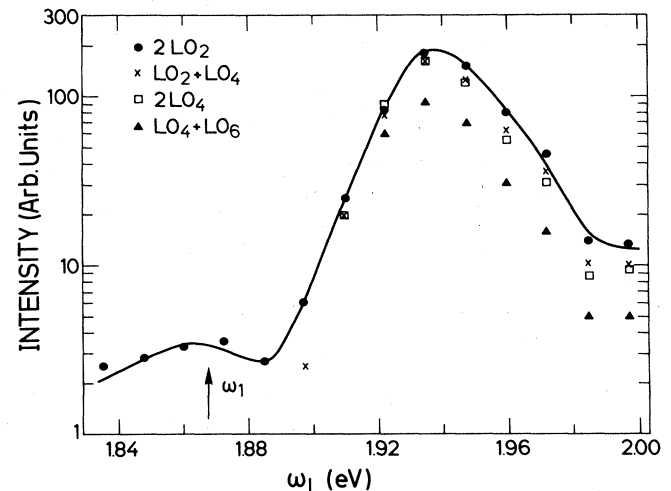


FIG. 3. Resonance of the Raman efficiency for some of the phonon combinations shown in Fig. 2. No absorption correction has been applied.

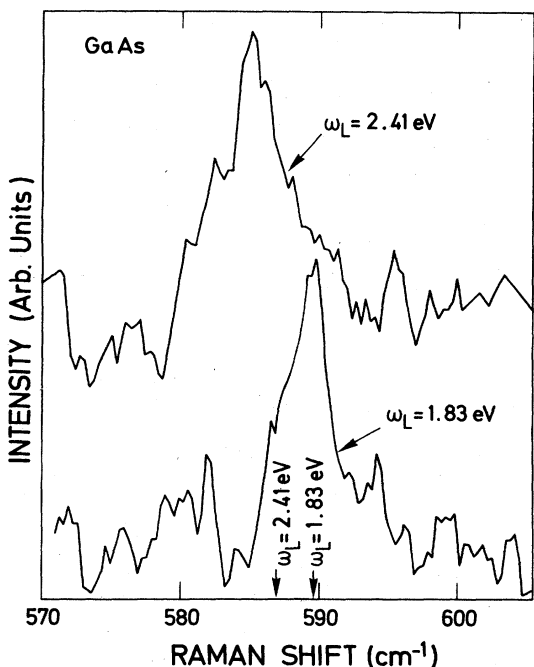


FIG. 4. Two-LO-phonon Raman spectrum of bulk GaAs (temperature  $\sim 10$  K) for two different laser energies. The arrows denote the calculated peak positions.

been observed in bulk GaAs.<sup>11</sup> In Fig. 4 we show two-LO-phonon spectra of bulk GaAs for laser energies close and far above the  $E_0 + \Delta_0$  gap ( $\sim 1.85$  eV). Although the peaks are very weak compared with those of the superlattices, a relative shift of  $\sim 5$   $\text{cm}^{-1}$  is apparent. The arrows show

theoretical predictions using Zeyher's theory,<sup>3</sup> assuming that the dominant contribution arises from the  $E_0 + \Delta_0$  gap and taking  $M_{\text{LO}} = 530$  as the "effective" LO-phonon mass.<sup>11,12</sup> The reason for the decrease of the peak energy is that the double-resonance process, which dominates the Raman efficiency, implies a real transition between two electronic states with emission of a phonon. Because the electronic bands display a parabolic dispersion, when the laser energy increases larger phonon wave vectors are needed to keep the electronic transition real. These larger phonon wave vectors correspond to lower phonon frequencies, as can be seen in the phonon dispersion curves for the LO branch.<sup>12</sup> Hence we believe that all phonon combinations are present in the second-order spectrum out of resonance but shifted with respect to the values calculated from Fig. 1. They cannot be clearly resolved due to the larger slit width used to detect this weak spectrum. The off-resonance spectrum in the  $z(x,x)\bar{z}$  configuration is also similar to the  $\Gamma_1$  component of the second-order spectrum of bulk GaAs,<sup>13</sup> thus suggesting that the second-order electron-phonon Hamiltonian (deformation potential) also plays an important role.

In summary, we have reported the most prominent features of the second-order Raman spectrum of GaAs-AlAs superlattices, which in resonance are determined by the Fröhlich electron-phonon interaction. Second-order Raman structure induced by the deformation potential interaction is also seen out of resonance. This opens up the interesting possibility of studying the effect of zone folding (in particular, the folding of the acoustic branches) on the two-phonon density of states.

The technical assistance of M. Siemers, H. Hirt, and P. Wurster is gratefully acknowledged. We thank A. Fischer for his help in growing the superlattices.

\*On leave from Materials Science Laboratory, Reactor Research Centre, Kalpakkam 603102, India.

<sup>1</sup>M. Cardona, in *Light Scattering in Solids II*, edited by M. Cardona and G. Güntherodt, Topics in Applied Physics, Vol. 50 (Springer, Berlin, 1982), p. 19, and references therein.

<sup>2</sup>Except in impurity-induced Raman scattering. See A. A. Gogolin and E. I. Rashba, *Solid State Commun.* **19**, 1177 (1976).

<sup>3</sup>R. Zeyher, *Phys. Rev. B* **9**, 4439 (1974).

<sup>4</sup>B. A. Weinstein and M. Cardona, *Phys. Rev. B* **8**, 2795 (1973).

<sup>5</sup>J. Menéndez, M. Cardona, and L. K. Vodopyanov, *Phys. Rev. B* **31**, 3705 (1985).

<sup>6</sup>W. Kauschke and M. Cardona (unpublished).

<sup>7</sup>B. Jusserand, D. Paquet, and A. Regreny, *Phys. Rev. B* **30**, 6245 (1984); C. Colvard, T. A. Grant, M. V. Klein, R. Merlin, R. Fischer, H. Morkoc, and A. C. Gossard, *ibid.* **31**, 2080 (1985).

<sup>8</sup>A. K. Sood, J. Menéndez, M. Cardona, and K. Ploog, *Phys. Rev. Lett.* **54**, 2111 (1985).

<sup>9</sup>A. K. Sood, J. Menéndez, M. Cardona, and K. Ploog, *Phys. Rev. Lett.* **54**, 2115 (1985).

<sup>10</sup>G. Kanellis, J. F. Morhange, and M. Balkanski, *Phys. Rev. B* **28**, 3406 (1983). This result, obtained from a microscopic lattice-dynamics approach, implies a vanishing of the phonon displacements at the interface, and differs from the macroscopic electrostatic model of R. Fuchs and K. L. Kliewer, *Phys. Rev.* **140**, A2076 (1965). A discussion of this problem is given in Ref. 8.

<sup>11</sup>D. Olego and M. Cardona, *Solid State Commun.* **39**, 1071 (1981).

<sup>12</sup>G. Dolling and J. L. T. Waugh, in *Lattice Dynamics*, edited by R. F. Wallis (Pergamon, London, 1965), p. 19.

<sup>13</sup>R. Trommer and M. Cardona, *Phys. Rev. B* **17**, 1865 (1978).